

# A Novel Approach for Studying Hydraulic Fracturing Success Factors beyond Brittleness Indices

Samnejad, M.

*Petroleum Engineering, University of Southern California, Los Angeles, CA, USA*

Aminzadeh, F. and Jha, B.

*Petroleum Engineering, University of Southern California, Los Angeles, CA, USA*

Copyright 2018 ARMA, American Rock Mechanics Association

This paper was prepared for presentation at the 52<sup>nd</sup> US Rock Mechanics / Geomechanics Symposium held in Seattle, Washington, USA, 17–20 June 2018. This paper was selected for presentation at the symposium by an ARMA Technical Program Committee based on a technical and critical review of the paper by a minimum of two technical reviewers. The material, as presented, does not necessarily reflect any position of ARMA, its officers, or members. Electronic reproduction, distribution, or storage of any part of this paper for commercial purposes without the written consent of ARMA is prohibited. Permission to reproduce in print is restricted to an abstract of not more than 200 words; illustrations may not be copied. The abstract must contain conspicuous acknowledgement of where and by whom the paper was presented.

**ABSTRACT:** The success of hydraulic fracturing jobs is often related to rock brittleness indices, which are taken as the sole impact factor determining fracturing results. Indeed, hydraulic fractures play a principal role in producing from low-permeability reservoirs; however, brittleness is not the only parameter contributing to productivity of unconventional resources. Under a variety of circumstances, brittleness indices are insufficient to explain rock fracability and permeability enhancement during hydraulic stimulation. For better prediction and design, it is imperative to identify and understand other factors affecting fracture creation and propagation, and to build models that include the effect of these factors on flow enhancement. To numerically model permeability enhancement after injection, we can regard fractured rock as a damaged continuum, which allows simulation of the deformation and fracturing response of the reservoir using material constitutive laws for brittle and ductile regions. We outline a coupled flow-geomechanical simulation framework that fits into available reservoir simulation platforms and does not require pre-specified fracture paths. We develop the fracture growth mechanisms for the coupled simulation framework by analyzing the effect of rock properties and in-situ stresses on the fracture length at different injection pressures. Based on these mechanisms, we propose factors that quantify the success of hydraulic fracturing jobs beyond the simplified rock brittleness indices.

## 1. BACKGROUND

United States has benefited economically from the boom in horizontal drilling and hydraulic fracturing technology, which rendered the development of domestic unconventional energy resources possible. US production of liquid fuels surpassed the Middle East in 2013 [Yo and Neff, 2014], adding 169,000 jobs between 2010 and 2012 [Brown and Yucel, 2013]. Reducing a country's dependence on the imported energy helps mitigate economic losses caused by foreign oil supply disruptions [Brown and Huntington, 2009].

The success of investment decisions pertaining to the exploitation of unconventional resources depends strongly on the reliability of models making predictions of post-stimulation performance. However, due to a lack of models based on accurate knowledge of the reservoir and rigorous understanding of the governing physics, there is a technology gap between the current models of stimulation and the field observations in the E&P industry.

A major drawback associated with common hydraulic fracturing simulation methods is that they need prior

knowledge on the fracturing path, meaning the outcome of the stimulation job should be fed as input to the model, rather than obtained as output. In addition, prevalent approaches for modeling performance of hydraulic fracturing jobs often fail to quantify the job results realistically, as linear elasticity and rock brittleness are the main underlying assumptions of most models. It has been shown, however, that there are a number of influence factors that need to be accounted for in prediction models. Brittle materials demonstrate a shorter period of ductile deformation before failure, which does not necessarily guarantee easier fracturing at lower ultimate rock strength values. Bai, 2016 states that, in fact, certain ductile formations may break at lower downhole pressures based on field measurements. Papanastasiou, 1997 incorporated the effect of plasticity in hydraulic fracturing using a cohesive crack model, showing that ductile rock behavior can lead to higher resulting fracture width values, while creating fractures with a smaller length. These observations suggest that limiting our target rocks and prediction models to linear elastic materials leads to inaccurate conclusions, since both mechanisms of brittle and ductile fracturing need to be considered for better modeling purposes.

The importance of confining stresses is emphasized by **Ashby and Sammis, 1990**, where it is shown that prevailing models of brittle fracture growth fail to accurately predict fracturing at higher confining stresses, where the fracturing process slows down. **Peach and Spiers, 1995** investigate, experimentally, the effect of plastic deformation on fluid transport properties, observing that while porosity increases rather steadily with strain, permeability changes are more complex to model when the rock undergoes elastoplastic deformation.

Considering the diversity of influence factors playing roles in hydraulic fracturing processes, as well as geological and geometrical complexities of reservoir property distribution, it is imperative to develop mathematically rigorous and numerically efficient models to make more reliable predictions and optimize design. Several attempts have been made for this purpose, which we briefly outline hereunder.

Traditional methods of bi-wing hydraulic fracture growth are applicable only under oversimplified conditions of homogeneous reservoir properties and planar fracture geometry (**Nordgren, 1972**). Discrete Fracture Network (DFN) models are capable of handling more complex fracture network geometries in the reservoir (**McClure et al., 2015**). Distinct Element Models (DEM) (**Zhao et al., 2014; Zanganeh et al., 2015**) and Interface Element Models with the penalty multiplier approach (**Ferronato et al., 2008**) and the Lagrange multiplier approach (**Jha and Juanes, 2014; Franceschini et al., 2016; Jha, 2016**), where faults and fractures are modeled as interface elements have also been proposed. However, these methods require prescribed fracture growth paths in the model. This means that the fracture can grow on pre-defined planes only. Certain other approaches, such as Cohesive Zone Elements (CZE) (**Gens et al., 1988**) represent fractures as planes of discontinuity and let fractures grow with time along the element boundaries. However, these methods impose a mesh dependency in the solution (**de Borst et al., 2004**) because the geometry of the propagation problem needs to be changed at each time step. Extended Finite Element Methods (XFEM) (**Mohammadnejad and Khoei, 2013; Khoei and Mohammadnejad, 2016; Fumagalli and Scotti, 2013**) addresses this problem by allowing the fractures to propagate across element boundaries, but the applicability of such methods to field-scale petroleum reservoir simulations is yet to be proven due to their computational cost and significant differences from commercial reservoir simulators currently used in the industry.

In this paper, we propose to study reservoir post-stimulation flow behavior by numerically simulating rock permeability enhancement from hydraulic fracturing while considering variable rock mechanical properties and reservoir in-situ conditions. We model the rock and

evolution in its poromechanical properties using the principles of Continuum Damage Mechanics (CDM), which has proven promising for geothermal applications (**Pogacnik et al., 2016**). The extension of our methodology proposed previously (**Samnejad et al., 2017**) exhibits the benefits of applying CDM approaches to model hydraulic stimulation of unconventional reservoirs and quantify various factors affecting the success of hydraulic fracturing jobs. Our technique has the advantage of fitting into available coupled simulators of flow and geomechanics, overcome the mesh dependency problem existing in previous methods, and honor principles of fracture mechanics for brittle rocks and plastic damage growth for rock ductility.

## 2. MATHEMATICAL FORMULATION

In this paper, we aim to show how we can build a comprehensive hydraulic fracturing model that can later be fit into coupled flow and geomechanical platforms. It is, therefore, useful to discuss the numerical simulation applications of our model.

If we regard this problem from a reservoir engineering standpoint, the domain is divided into volumetric elements and each element is undergoing changes in the stress state due to pressurized fluid flow across the element. Within each element, continuum damage mechanics principles can be used to describe the variations of reservoir parameters. Sections 2.1 through 2.2 further elaborate on this.

### 2.1 Governing Equations of Reservoir Multi-physics Processes

In order to simulate hydraulic fracturing processes, multiple physical phenomena need to be modeled. Well stimulation jobs include fracture initiation and propagation in a subsurface environment under tectonic stresses, leading to enhancement of rock permeability. Therefore, we present this complex problem as a coupled flow and geomechanics simulation framework, incorporating fracturing processes within each volume element of the grid.

- Fluid Conservation

In presence of geomechanical deformation, Darcy flow of a single-phase compressible fluid in the reservoir can be described as:

$$\left( \frac{\alpha - \Phi}{K_s} + \frac{\Phi}{K_f} \right) \frac{\partial p}{\partial t} + \alpha \frac{\partial \varepsilon_v}{\partial t} + \nabla \cdot \left[ \frac{k}{\mu} (-\nabla p + \rho_f g) \right] - Q_p = 0 \quad (1)$$

where  $\alpha$  is the Biot coefficient,  $\phi$  is porosity,  $K_s$  and  $K_f$  are bulk moduli for the solid and fluid phases respectively,  $p$  is pressure,  $t$  is time,  $\varepsilon_v$  is the volumetric strain,  $k$  is the

rock permeability tensor,  $\mu$  is the dynamic fluid viscosity,  $\rho_f$  is the fluid density,  $\mathbf{g}$  is the gravitational acceleration vector, and  $Q_p$  is the source term due to injection in the volume element.

It should be noted that when solving this equation to model hydraulic fracturing processes, the rock properties cannot be assumed constants and should be updated as functions of stress at each time step. This is in contrast to traditional reservoir simulations with constant permeability, porosity, and Young's modulus.

- Mechanical Equilibrium

For quasi-static deformation, the mechanical equilibrium equations can be written as the following:

$$\nabla \cdot \boldsymbol{\sigma} + \rho \mathbf{g} = \mathbf{0} \quad (2)$$

in which  $\boldsymbol{\sigma}$  is the total stress tensor, and  $\rho$  is the bulk density. The total stress tensor can be related to the effective stress tensor,  $\boldsymbol{\sigma}'$ , with the following equation:

$$\boldsymbol{\sigma}' = \boldsymbol{\sigma} + \alpha \rho \mathbf{I} \quad (3)$$

where  $\mathbf{I}$  is the identity matrix. The effective stress tensor is related to the strain tensor using the material constitutive laws. We assume that normal stresses are positive under tension.

## 2.2 Continuum Damage Mechanics Model for Element Behavior

We use a continuum damage mechanics workflow for modeling the change of hydromechanical properties of the rock, namely, permeability and stiffness, which influence the coupled behavior of flow and geomechanics. In our workflow, a pre-existing set of micro-inclusions within each 2D representative volume element can extend under bi-axial loads caused by fluid injection. Linear extensions of such micro-inclusions lead to increase in flow permeability and change in material stiffness. Figure 1 schematically shows a single crack inside a 2D element.

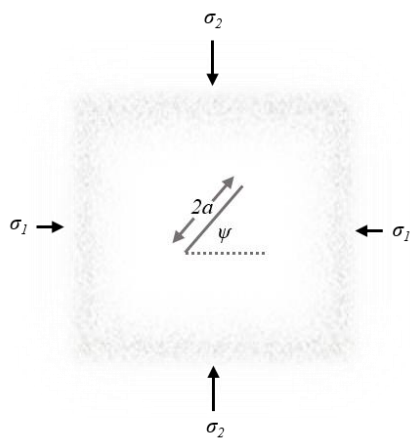


Figure 1. Schematic view of a volumetric element

To capture the overall effect of existence of  $N$  different families of cracks in the element, with  $m_k$  members in  $k$ th family, we define a damage parameter that sums up the relative lost surfaces associated with individual cracks of each family,

$$D = \sum_{k=1}^N m_k \left( \frac{a}{a_c} \right)^2 (\mathbf{n} \otimes \mathbf{n}) \quad (4)$$

where  $\mathbf{n}$  denotes the normal vector to the crack plane, and  $a_c$  is the critical crack half-length above which unstable crack growth occurs.

It is important to note that damage parameter evolution, which depends on crack extension, controls permeability enhancement. Therefore, if we capture crack extension properly, we would be able to forecast reservoir post-stimulation performance.

We use principles of brittle fracture mechanics and ductile damage growth to trace the evolution of crack lengths. For simplicity, we assume one crack family per element with one member in the family i.e.  $N=1, m_k=1$ .

In contrast to common approaches, which overlook non-brittle inelastic crack growth, we include multiple mechanisms of brittle and ductile crack propagation. The following discussion elaborates on this.

- Brittle crack growth

Classical fracture mechanics principles assume that the bulk behavior of the medium can be described with linear elasticity. **Griffith, 1921** developed the concept of the stress intensity factor,  $K_I$ , to predict the stress,  $\sigma$ , near the tip of a crack with half-length  $a$ .

$$K_I = \sigma \sqrt{\pi a} \quad (5)$$

A pre-existing crack grows until  $K_I$  becomes equal to a critical value  $K_{IC}$ , fracture toughness, which is assumed to be a material property.

$$K_I = K_{IC} \quad (6)$$

For brittle rocks containing cracks under increasing local tensile loads, **Shao et al., 2004** propose a model for crack propagation, in which increasing the fluid pressure acts as an opening force on the crack plane extending its length by opposing normal compressive forces.

$$K_I = (\sigma_n + p + f(a)\sigma_t)\sqrt{\pi a} \quad (7)$$

The amount of macroscopic deviatoric stress is translated to the local tensile stress using a scalar factor  $f(r)$ , where  $r$  is the relative crack length with respect to the critical crack length,  $2a_c$ . Figure 2 shows the evolution of the  $f$  function we have chosen, aiming to attenuate sliding effects as the critical crack length is approached. For practical purposes, this function can be approximated

from calibration with experimental rock failure data or numerical micromechanical analyses.

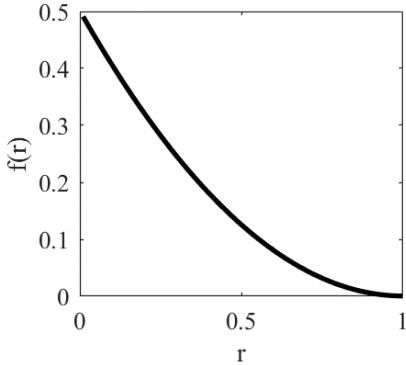


Figure 2. Variation of scalar function  $f(r)$  with relative crack length  $r$

- Ductile crack growth

Since classical fracture mechanics principles fail to give a proper view of fracture growth in a broad range of rock types; prevalent hydraulic fracturing simulation approaches only consider brittle crack growth. This often leads to overestimations of fracture length and stimulated reservoir volume if the rock exhibits ductility.

Crack growth on the plastic yield surface, can be quantified by use of a constitutive relation between the plastic strain and the crack length (**Shojaei et al., 2014**). We use a simplified form of the proposed equation as follows:

$$a_i = a_{i0} + \chi \left( \frac{a_i}{a_{i0}} \right) (a_{ic} - a_{i0}) \sum_{k=0}^N \frac{|\Delta \varepsilon_p|_k}{\varepsilon_f}, \quad (8)$$

where  $a_i$  denotes the crack half-length in  $i$ th direction, and  $|\Delta \varepsilon_p|_k$  is the equivalent plastic strain increment at loading step  $k$  defined as:

$$|\Delta \varepsilon_p| = \sqrt{\frac{2}{3} \Delta \varepsilon_{p_{ij}} \Delta \varepsilon_{p_{ij}}} \quad (9)$$

We use a simplified power law constitutive model of plasticity to relate strain to stress, as shown in Equation 10 for uniaxial deformation.

$$\sigma - \sigma_{y0} = k \sigma_{y0} \varepsilon_p^n \quad (10)$$

where  $\sigma_{y0}$  is the yield stress,  $k$  is the power law multiplier, and  $n$  is the power law exponent. We found it more convenient in our applications to work with threshold pressure,  $P_t$ , as the onset of plastic yielding. See Equation 3 to see how it relates to stress. We demonstrate the effect of certain material properties on the crack growth beyond the elastic limit.

We neglect the changes of the final fracture strain,  $\varepsilon_f$ , with in-situ stresses and rearrange Equation (8) to solve for  $a_i$  explicitly:

$$a_i = \frac{a_0}{1 - \left( \frac{\chi}{a_{ic}} \right) (a_{ic} - a_{i0}) \left( \frac{\sum_{k=0}^N |\Delta \varepsilon_p|_k}{\varepsilon_f} \right)} \quad (11)$$

One may note that the initial crack length after the onset of plastic yielding is, in fact, the maximum crack length achieved during linear elastic deformation.

Incorporating rock ductile behavior introduces nonlinearity to the problem. It enables us to go beyond existing linear elastic fracture mechanics approaches and quantify fracturing processes in formations that exhibit brittle fracturing only partially. Section 3 provides an insight on a number of important impact factors that are often overlooked in common analyses of fracturing processes.

### 3. MULTI-MECHANISM CRACK GROWTH MODELING

We use the material presented in the discussion section above to illustrate the evolution of brittle crack lengths within each volume element with increasing borehole pressure to better understand the parameters that influence the creation of fractures in the reservoir, and ultimately, permeability enhancement as a result of fluid injection.

Table 1 summarizes the reference parameters that we have used for brittle fracture growth, based on data in part provided by **Gowd and Rummel, 1980** for sandstone. Table 2 is a similar list of parameters when the increasing pressure in the wellbore corresponds to a rising stress field above yield strength of the rock.

We identified five important factors that can control the growth of cracks in the reservoir in addition to simplified brittleness indices: alignment of inclusions, confinement load, load biaxiality (triaxiality in 3D), degree of ductility, and the onset pressure of yield. Sections 3.1 through 3.5 elaborate on these by showing plots of the extension of crack lengths,  $a$ , with respect to the injection pressure considering different impact factors.

#### 3.1 Pre-existing Cracks Orientation

Rocks undergo numerous geological processes, which lead to preferred orientation of their inclusions and flaws. These flaws bear portions of the remote stress field depending on their orientation as shown in equations 6 through 9. Therefore, understanding the initial crack orientation helps better quantify hydraulic fracturing job results.

The effect of initial crack orientation is shown in Figure 3, where the propagated crack half-length is plotted against the injection pressure. Considering the maximum principal stress being in the vertical direction (see Table

1), the initial cracks are expected to prefer the vertical alignment to the horizontal alignment ( $\psi \geq 45^\circ$ ).

As expected, the higher the number of cracks aligned normal to the minimum principal stress direction, the faster is crack propagation, i.e., the cracks reach a certain value of half-length at lower injection pressures. In this work, we have not included the effect of fracture re-orientation with respect to the minimum principal stress, but it can be studied using models as presented in **Ashby and Sammis, 1990**.

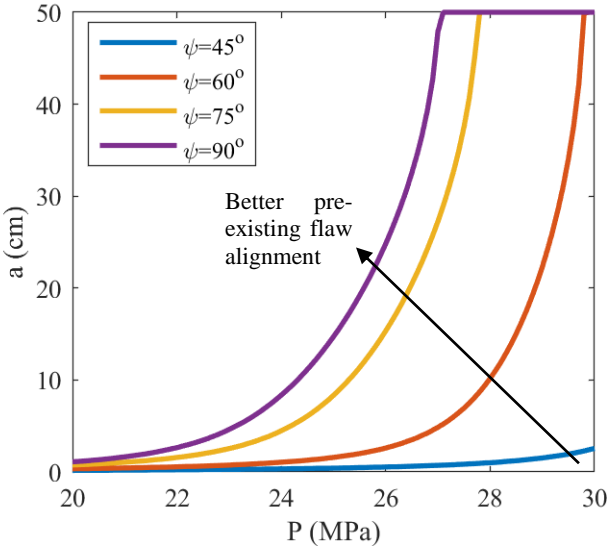


Figure 3. Pre-existing crack orientation effect on brittle crack growth

### 3.2 In-situ Stress Magnitude

Besides transition to ductile behavior, in-situ stresses play an important role in the design and outcome of hydraulic fracturing (**Samnejad et al., 2017**). Higher confining stresses impose larger compression on the crack faces against each other thereby preventing further growth. Therefore, hydraulic fracturing in deep formations can be very challenging due to very high downhole pressures required for growth.

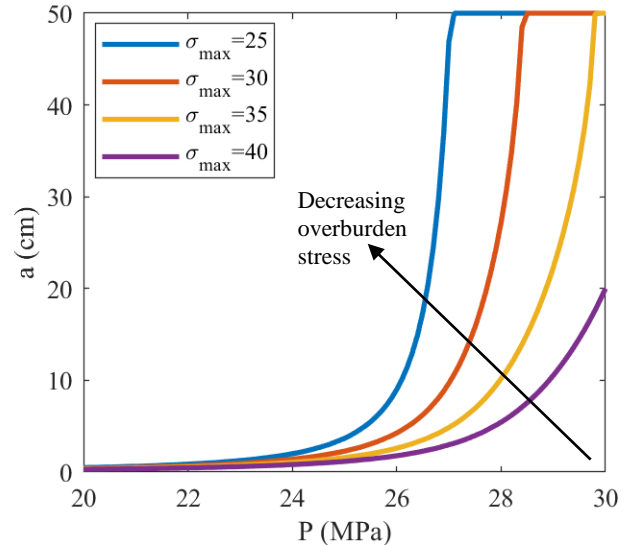


Figure 4. Maximum principal stress effect on brittle crack growth

Figure 4 shows the impact of maximum principal stress on brittle crack growth. To avoid redundancy, another figure for minimum principal stress is not included since the impact is similar. In general, lower magnitudes of in-situ stresses allow easier fracturing in brittle rocks. As can be seen on the plot, 15 MPa of stress drop results in significant crack growth stimulation. This observation can have important implications when identifying suitable fracturing intervals. Rocks behaving the same in the lab may not exhibit similar fracturing behavior in the field, i.e. under different loads.

### 3.3 In-situ Stress Anisotropy

We analyze the stress anisotropy effect by looking into the stress anisotropy ratio,  $\lambda$ , defined as the ratio of the two principal stress magnitude values:

$$\lambda = \frac{\sigma_{max}}{\sigma_{min}} \quad (12)$$

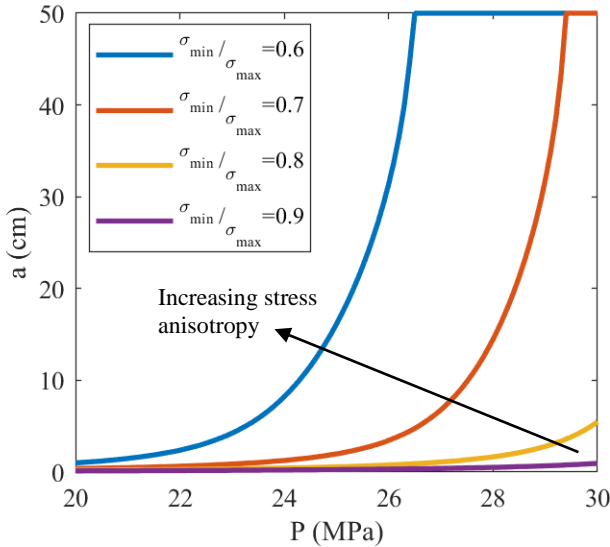


Figure 5. In-situ stress anisotropy effect on brittle crack growth

Stress biaxiality (increasing  $\lambda$ ) has negative effects on crack growth, and presence of larger stress anisotropy could contribute to better fracture development. Note that if the minimum principal stress becomes comparable to the maximum principal stress, the compressional forces of crack closure become dominant, and higher pumping pressures will be required to initiate noticeable crack growth.

### 3.4 Degree of Ductility

It has been shown experimentally that permeability can improve up to an order of magnitude during ductile deformation (**Colin et al., 1995**). This motivates us to understand the crack growth mechanism associated with plasticity. Here, we demonstrate that although a crack propagates more slowly on the yield surface compared to the linear elastic domain, the process of irreversible fracturing continues.

In Figure 6, the closer the  $n$  exponent is to unity, i.e. linearity, the higher is the crack growth inside the medium. Note that a bottomhole pressure of 30 MPa is assumed to be the onset of plastic yielding.

At lower pressures, linear elastic material models are sufficient to explain deformation and fracturing phenomena. After the onset of plastic yielding, depending upon the degree of rock ductility, fracture growth process slows down to a certain extent.

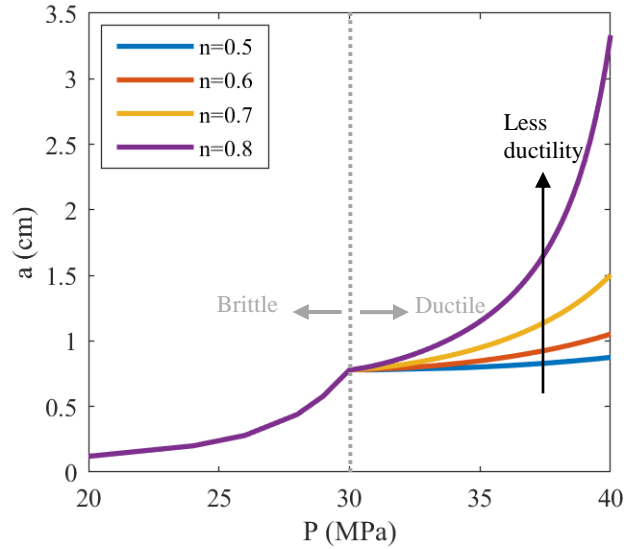


Figure 6. Ductility effect on plastic crack growth

### 3.5 Yield Stress

If the rock yields after large effective loads are imposed, then plastic strain only happens at very high pressures, and a substantial portion of the crack growth occurs in a brittle manner leading to higher ultimate crack lengths. This can be shown by plotting the effect of threshold pressure,  $p_t$ , below which rock behaves elastically, on crack growth (Figure 7).

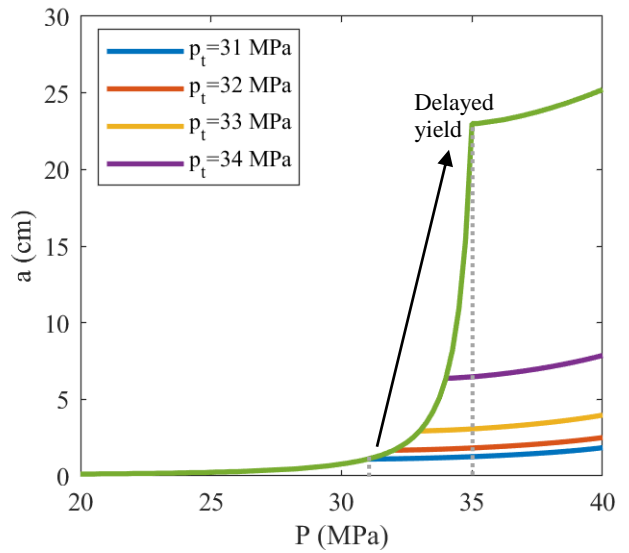


Figure 7. Effect of the threshold pressure on plastic crack growth

## 4. OPERATIONAL IMPLICATIONS OF IMPACT FACTORS

In this section, we demonstrate how the factors analyzed in Section 3 can dictate operational conditions that are required to obtain desirable fracture growth. More specifically, we are analyzing the relative extension of created fractures with respect to their original length,  $a_i$ , under a given set of reservoir and operational conditions.

### 4.1 Pre-existing Cracks Orientation

Fractures oriented in optimum directions, i.e. perpendicular to the minimum principal stress, can grow more rapidly compared to other fractures. This can be seen in Figure 8, where even at relatively lower pressures, fractures of extended length are formed, primarily because of their preferred direction. Note that we assume an initial crack length of 1 mm and a critical length of 50 cm (Table 1).

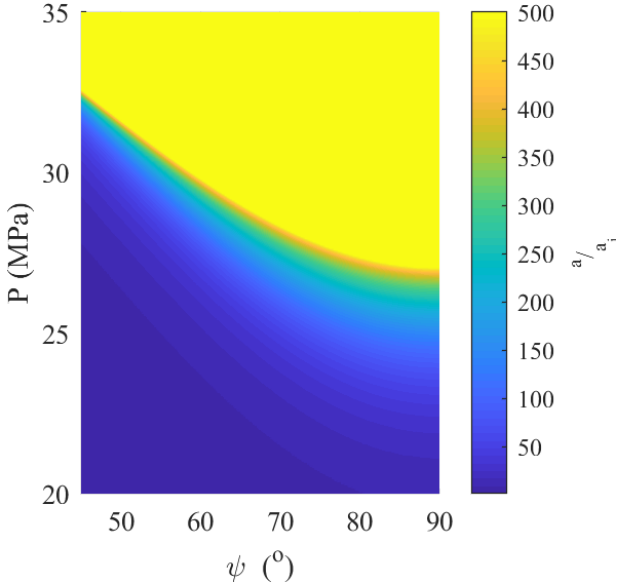


Figure 8. Effect of the direction of pre-existing inclusions on the required injection pressure

### 4.2 In-situ stress magnitude

Hydraulic fracturing operations in highly confined media can be very challenging because the required pumping pressure to create fractures with desired length increases with the in-situ stress magnitude. Figure 9 shows this phenomenon, where only increasing values of pressure can cancel out the effect of high overburden loads. A similar trend is expected to be observed for the minimum principal stress, which is not included here to avoid redundancy.

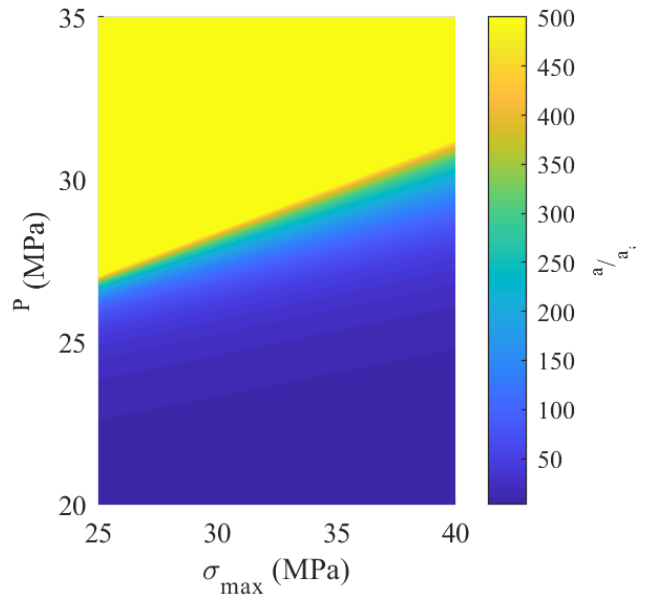


Figure 9. Effect of the magnitude of in-situ stress on the required injection pressure

### 4.3 In-situ Stress Anisotropy

We emphasize on the observation made in section 3.3 by showing how increasing stress biaxiality imposes higher required injection pressures to achieve desired fracture length. Figure 10 shows the dependency.

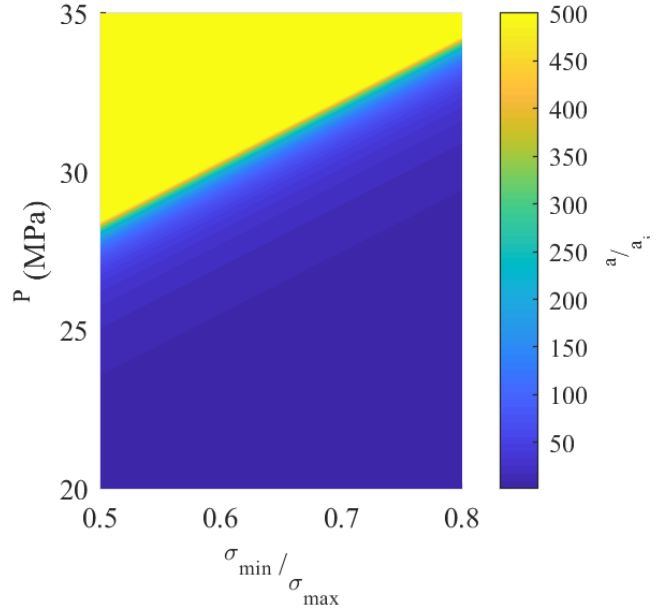


Figure 10. Effect of stress anisotropy on the required injection pressure. Lower values on the x-axis indicates higher anisotropy.

### 4.4 Degree of Ductility

To better demonstrate the effect of rock ductility on required injection pressures, we have chosen an early transition of the rock fracturing behavior from brittle to ductile, at an injection pressure of 30 MPa, when not much brittle crack extension has taken place. Figure 11

shows that for a predominantly ductile rock, even high pressurization cannot cause significant crack coalescence. This phenomenon is less pronounced when the rock exhibits less ductility (higher  $n$  value).

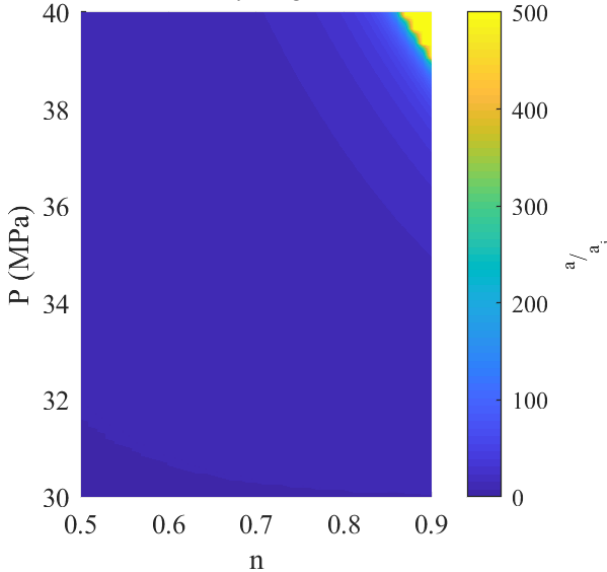


Figure 11. Effect of the rock ductility parameter on the required injection pressure

#### 4.5 Yield Stress

Early transition to ductile behavior prevents rapid crack extension. We show that for small values of the threshold pressure, i.e. the pressure at which the rock yields, crack extension occurs very slowly due to ductile transition. On the contrary, if the major portion of crack growth happens in the brittle region, i.e. a higher threshold pressure, rock breaks at even low injection pressure. Figure 12 depicts this phenomenon.

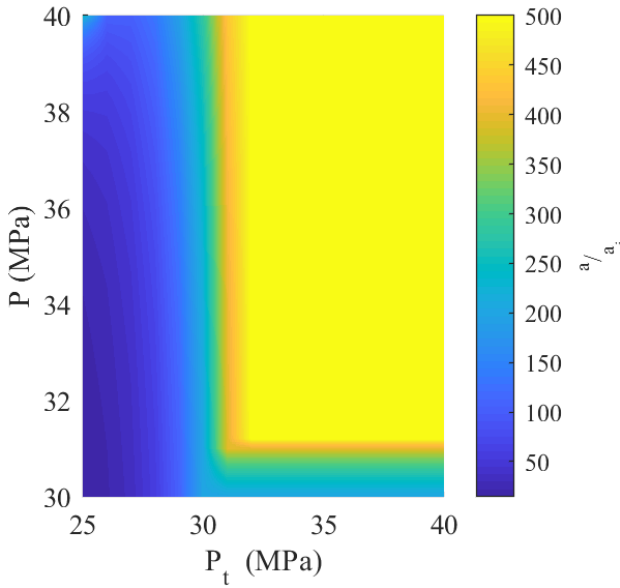


Figure 12. Effect of the threshold pressure on the required injection pressure

## 5. CONCLUSIONS

We identified and quantified the impact of a number of rock mechanical and in-situ parameters on fracture propagation during hydraulic fracturing. These effects have not been addressed in existing models of fracturing job success prediction. We developed a multi-mechanism model of crack growth that incorporates the effects of these factors on the fracture length and the required injection pressure, both of which determine the success of a hydraulic fracturing job.

Our model is advantageous over existing DFN model-based approaches because it does not require prior knowledge of the location and path of created fractures since it predicts the growth of fractures. Our model is capable of incorporating multiple mechanisms of fracture propagation arising from multiple independent rock properties and in-situ stress conditions. Since we use a continuum damage mechanics approach, our model does not encounter mesh dependency problems during numerical simulations.

We conclude that the initial alignment of pre-existing inclusions, absolute and relative magnitudes of in-situ stresses, degree of ductility, and plastic yield stress are important factors that contribute to growth of fractures and, therefore, to success of hydraulic fracturing jobs.

Future work is aimed at implementing our model into a numerical simulator to demonstrate the applicability of our method to reservoir-scale simulations and highlight the robustness of workflow.

## 6. TABLES

Table 1. Reference parameters used for modeling brittle crack growth

Parameter	Nomenclature	Value
Biot coefficient	$\alpha$	0.9
Crack orientation	$\psi$	60°
Fracture toughness	$K_{IC}$	0.7 MPa $\sqrt{m}$
Initial crack half-length	$a_0$	1 mm
Critical crack half-length	$a_c$	50 cm
Young's modulus	$E$	100 GPa
Poisson's ratio	$\nu$	0.2
Horizontal Stress	$\sigma_1$	25 MPa
Vertical Stress	$\sigma_2$	35 MPa

Table 2. Reference parameters used for modeling ductile crack growth

Parameter	Nomenclature	Value
Biot coefficient	$\alpha$	0.9
Crack orientation	$\psi$	45°
Power law exponent	$n$	0.7
Power law multiplier	$k$	2

Proportionality factor	$\chi$	1
Fracture Strain	$\varepsilon_f$	0.05
Initial crack half-length	$a_e$	max @ brittle
Critical crack half-length	$a_c$	50 cm
Threshold pressure	$p_t$	30 MPa
Horizontal Stress	$\sigma_1$	25 MPa
Vertical Stress	$\sigma_2$	40 MPa

## REFERENCES

- Ashby, M.F., C.G. Sammis. 1990. The damage mechanics of brittle solids in compression. *Pure and applied geophysics.*, 133: 489 – 521.
- Bai, M. 2016. Why are brittleness and fracability not equivalent in designing hydraulic fracturing in tight shale gas reservoirs. *Petroleum*. 2: 1–19.
- Brown, S.P., and H.G. Huntington. 2009. Estimating U.S. Oil Security Premiums. *Energy Modeling Forum of Stanford University, Stanford, CA, September 2009*
- Brown, S.P., and M. Yucel. 2013. The Shale Gas and Tight Oil Boom: U.S. States' Economic Gains and Vulnerabilities. *Council on Foreign Relations, New York, NY, October 2013*
- de Borst, R., Gutierrez, M. A., Wells, G. N., Remmers, J. J. C., Askes, H. 2004. Cohesive-zone models, higher-order continuum theories and reliability methods for computational failure analysis, *Int. J. Num. Methods Eng.*, 60: 289–315, doi:10.1002/nme.963
- Ferronato, M., G. Gambolati, G. Janna, and P. Teatini. 2008. Numerical modeling of regional faults in land subsidence prediction above gas/oil reservoir. *Int. J. Numer. Anal. Meth. Geomech.* 32: 633–657.
- Franceschini, A., M. Ferronato, C. Janna, and P. Teatini. 2016. A novel Lagrangian approach for the stable numerical simulation of fault and fracture mechanics, *J. Computational Phys.*, 314, 503–521
- Fumagalli, A. and A. Scotti. 2013. A numerical method for two-phase flow in fractured porous media with non-matching grids. *Adv. Water Resour.*, 62: 454-464.
- Gens, A., I. Carol, and E.E. Alonso. 1988. An interface element formulation for the analysis of soil-reinforcement interaction. *Comput. Geotech.* 7: 133–151.
- Gowd, T.N., and F. Rummel. 1980. Effect of confining pressure on the fracture behavior of a porous rock. *Int. J. Rock Mech. Min. Sci. and Geomech.*, 17: 225–229.
- Griffith, A.A. 1921. The phenomena of rupture and flow in solids. *Philosophical Transactions of the Royal Society of London*, 221: 163–198.
- Jha, B. 2016. Evolution of stress transfer mechanisms during mechanical interaction between hydraulic and natural fractures. *J. Sustainable Energy Eng.*, 4: 296 – 309.
- Jha, B., and R., Juanes. 2014. Coupled multiphase flow and poromechanics: A computational model of pore pressure effects on fault slip and earthquake triggering. *Water Resour. Res.*, 50: 3776 – 3808.
- Khoei, A. R., N. Hosseini, and T. Mohammadnejad. 2016. Numerical modeling of two-phase fluid flow in deformable fractured porous media using the extended finite element method and an equivalent continuum model, *Adv. Water Resour.*, 94, 510-528
- McClure, M.W., M. Babazadeh, S., Shiozawa, J. Huang. 2015. Fully coupled hydromechanical simulation of hydraulic fracturing in three-dimensional discrete fracture networks. *SPE Hydraulic Fracturing Technology Conference, The Woodlands, TX, 3-5 February 2015*
- Mohammadnejad, T., and A.R. Khoei. 2013. Hydromechanical modeling of cohesive crack propagation in multiphase porous media using the extended finite element method. *Int. J. Numer. Anal. Methods Geomech.*, 37: 1247–1279.
- Nordgren, R.P. 1972. Propagation of a vertical hydraulic fracture. *Society of Petroleum Engineering Journal*. 12: 306 – 314.
- Papanastasiou, P. 1997. The influence of plasticity in hydraulic fracturing. *International Journal of Fracture*. 84: 61–79.
- Peach, C.J., and C. Spiers. 1995. Influence of crystal plastic deformation on dilatancy and permeability development in synthetic salt rock. *Technophysics*, 256: 101–128.
- Pogacnik, J., D. Elsworth, M. O'Sullivan, and J. O'Sullivan. 2016. A damage mechanics approach to the simulation of hydraulic fracturing/shearing around a geothermal injection well. *Computers and Geotech*, 71: 338–351.
- Popp, T. and H. Kern. 2001. Evolution of dilatancy and permeability in rock salt during hydrostatic compaction and triaxial deformation. *Journal of geophysical research*. 106: 4061–4078.
- Samnejad, M., B. Jha, and F. Aminzadeh. 2017. Permeability Enhancement Simulation using Coupled Flow and Continuum Damage Mechanics. *SPE Annual Technical Conference and Exhibition, San Antonio, TX, 9-11 October 2017*
- Samnejad, M., F. Aminzadeh, A. Bubshait. 2017. Acoustoelastic estimation of the in-situ stresses from sonic logs for a carbonate reservoir. *SPE Western Regional Meeting, Bakersfield, CA, 23-27 April 2017*
- Shao, J.F., Y.F. Lu, and D. Lydzba. 2004. Damage modeling of saturated rocks in drained and undrained conditions. *Journal of engineering mechanics*, 130: 733–740.
- Shojaei, A., A.D. Taleghani, and G. Li. 2014. A continuum damage failure model for hydraulic

- fracturing of porous rocks. *Int. J. of Plasticity*, 59: 199–212.
26. Yo, M., S., and Neff. 2014. Liquid Fuels and Natural Gas in the Americas. *EIA Energy Conference, Washington, DC, 14 July 2014*
  27. Zanganeh, N., E. Eberhardt, and R.M. Bustin. 2015. Investigation of the influence of natural fractures and in-situ stress on hydraulic fracture propagation using a distinct-element approach. *Can. Geotech. J.* 52: 926–946.
  28. Zhao, Q., Lisjak, A., Mahabadi, O., Liu, Q., Grasselli, G. 2014. Numerical simulation of hydraulic fracturing and associated microseismicity using finite-discrete element method. *J. Rock Mech. Geotech. Eng.*, 6: 574-581, doi:10.1016/j.jrmge.2014.10.003